

# Improving optical trapping in the axial direction and a continuous change of the optimal trapping depth

S.Nader S.Reihani<sup>1,2</sup>, and Lene B. Oddershede<sup>2</sup>

<sup>1</sup>Institute for Advanced Studies in Basic Sciences (IASBS), P.O.Box 45195-1159, Zanjan 45195, Iran

<sup>2</sup>Niels Bohr Institute, Blegdamsvej 17, 2100 Copenhagen, Denmark

## ABSTRACT

Oil immersion objectives have higher numerical aperture than water immersion objectives thus providing higher optical resolution. This is important for confocal microscopy as well as for the strength of an optical trap created by such an objective, because the efficiency of an optical trap is limited by its axial strength. However, light focused by oil immersion objectives suffer from spherical aberrations caused e.g. by a mismatch between the refractive index of the immersion and sample media. Such aberrations widen the intensity profile in the focal region thus restricting the axial resolution of the objective and decreasing the axial optical trapping strength. Objectives are typically designed such that the spherical aberrations are minimized for visible wavelengths and a few microns away from the surface. However, often optical traps are based on infrared lasers or are used further away from the surface thus introducing considerable spherical aberrations. We have shown that a tuning of the immersion refractive index can minimize the total spherical aberrations at any desired depth, thus maximizing the trapping efficiency and giving rise to optical trapping strengths twice as large as previously reported.<sup>15</sup> Changing the immersion media, however, is a discrete way of tuning the optimal trapping depth: An increment (decrement) of 0.01 in the refractive index of the immersion media gives rise to an increase (decrease) of  $\simeq 4\mu\text{m}$  and  $\simeq 10\mu\text{m}$  of the most efficient trapping depth for infinity-tube length and finite-tube length objectives, respectively. Here, we show that combining a change of immersion media with changing tube length provides a continuous way of changing the optimal trapping depth. Also, we show how trapping conditions change with polarization.

**Keywords:** optical tweezers, confocal microscopy, oil immersion objective, trapping efficiency, spherical aberration

Focusing a  $\text{TEM}_{00}$  laser beam by a well-corrected high numerical aperture objective lens produces a micron-scale 3-dimensional Gaussian intensity profile. If the gradient is steep enough to overcome scattering forces, this is termed an optical trap and can be used to trap and manipulate specimens like cells, bacteria and colloidal particles.<sup>2,3</sup> Also, optical traps have successfully been used as force-scopes measuring the force necessary to e.g. unfold nucleic acid structures.<sup>5,6</sup> The laser and the objective are the most important parts of optical tweezers. A common problem with using oil immersion objective lenses for optical tweezers (and confocal microscopy) is the presence of the optical aberrations. For optical trapping, the most important optical aberrations are termed spherical aberrations and they cause the strength of the optical trap to decrease as the depth within the sample is increased. Therefore, to achieve maximum efficiency of the trap in experiments using oil immersion objectives one has to perform the experiment close to the glass surface of the experiment chamber, where the experiments will suffer from the vicinity of this wall, potentially with dramatic effects. One main source of spherical aberrations is the mismatch of the refractive indices of the immersion media (oil) and specimen media (water), other sources include variation in coverglass-thickness, the tube length etc. The design of the objective lenses is such that the spherical aberrations are compensated for at specific visible wavelengths<sup>4</sup> and depths within the sample on the order of a few microns. Hence, the objectives are not optimal for using infrared trapping lasers, especially if trapping is performed away from the surface of the chamber. In aqueous samples, this effect can be nearly avoided by using water-immersion objectives. However, water immersion objectives have

---

Further author information:

S.N.S.R.: E-mail: reihani@iasbs.ac.ir ; reihani@nbi.dk

L.B.O.: E-mail: oddershede@nbi.dk

lower numerical apertures than obtainable with oil immersion: Theoretically, the numerical aperture of water immersion objectives can reach 1.33 and the highest numerical aperture presently available is around 1.2. In comparison, oil immersion objectives are presently available with a numerical aperture of 1.65. The higher the numerical aperture, the better the optical resolution of the objective, the stronger the optical trap.

It has been suggested to compensate the aberrations by altering the tube length of the microscope into which the tweezers potentially are implemented.<sup>7,8</sup> This has been experimentally proven in axial<sup>4</sup> and lateral<sup>9</sup> directions. However, in practice it is cumbersome, if not impossible, to continuously change the tube length of the microscope in which the tweezers are implemented. We have introduced a significantly simpler, easier and faster method to compensate the spherical aberrations, significantly improve optical trapping strength and provide optimal trapping conditions at any desired depth within the chamber.<sup>15</sup> This is done by adjusting the refractive index of the immersion media to the desired conditions. Changing immersion oil causes a discrete way of changing compensation depth, however, combining this technique with changing the tube length,<sup>4,9</sup> we here show that this provides a continuous way to reposition the optimal trapping depth in optical tweezers implemented in microscopes.

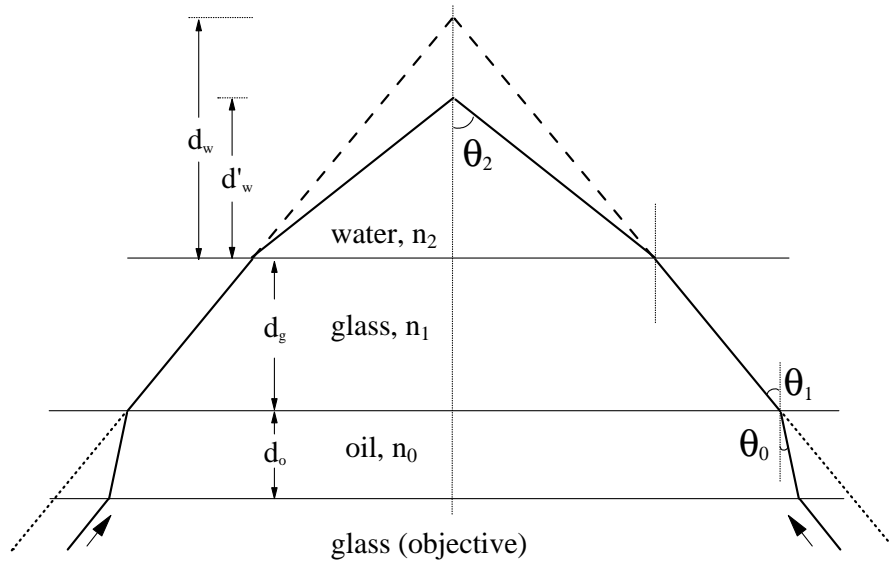
Our optical tweezer setup is based on a Nd – YVO<sub>4</sub> laser with wavelength 1064nm and is implemented in an inverted Leica microscope with a quadrant photodiode back focal plane detection scheme,<sup>10</sup> for a full description of the equipment see reference [11]. Data are acquired using a National Instruments Analog to Digital card (PCI-MIO-16E-4) and the sample is mounted on a two axis translational Piezoelectric stage (PI-731.20, Physik Instrumente) with capacitive feedback control and nanometer positioning resolution. Two different objectives were used for the experiments: An Infinity Tube Length Corrected objective (Leica, HCX PL Apo, 63X, NA 1.32,  $\infty$ , 0.17), and a Finite Tube Length Corrected objective (Leitz, PL Apo, 63X, NA 1.32, 170, 0.17), abbreviated ITLC and FTLC, respectively. The position time-series of the trapped beads were acquired using a custom-made LabView program and analyzed using a Matlab based power spectrum analysis program<sup>12</sup> to extract the corner frequency  $f_c$  and spring constant  $k$  of the the trap ( $k = 2\pi\gamma f_c$ ,  $\gamma$  being the drag coefficient of the trapped bead). To perform the most accurate measurements of the spring constant in the axial direction and to prevent an overestimation of the spring constant, measurements of bead positions in the axial direction were performed with the numerical aperture of the condenser set to 0.4.<sup>13,14</sup> For measurements of bead positions in the lateral direction the condenser aperture was fully opened. The output laser power was set 120 mW unless otherwise mentioned. Each data point in the graphs represents an average of 25 measurements (5 different beads, 5 measurements for each bead) and the error bars show the standard deviation of the results.

For an objective satisfying the sine condition and illuminated with a linearly polarized Gaussian laser beam the effect of the Spherical Aberrations (SA) on the 3-D Intensity Points Spread Function (IPSF) in the second medium can be accounted for by a phase factor.<sup>8</sup> In the case where the SA are caused by a mismatch between refractive indices of two media, the phase factor at depth  $d_w$  in the second medium is given by<sup>8</sup>

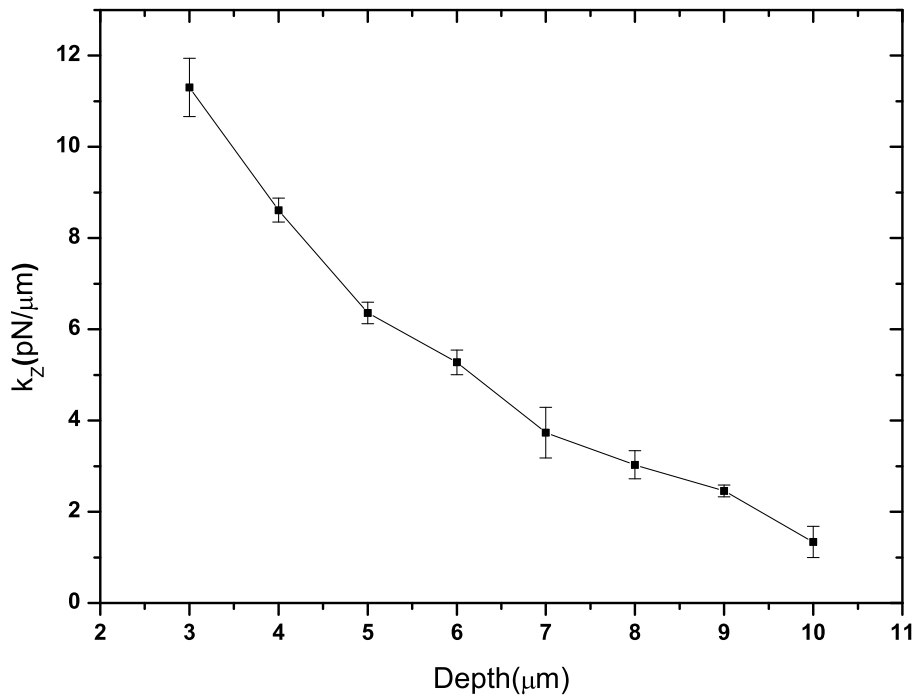
$$\psi(\theta_1, \theta_2, -d_w) = -k_0 d_w (n_1 \cos \theta_1 - n_2 \cos \theta_2), \quad (1)$$

where  $\theta_1$ ,  $\theta_2$ ,  $k_0$  and  $d_w$  are the incident and refracting angles in the first and second media, wave number in vacuum and the nominal trapping depth, respectively (see Figure 1). The intended focus depth of the objective,  $d_w$ , is deeper in the sample than the actual, aberrated, depth of the focus point,  $d'_w$ .

Figure 1 shows a schematic of the optical path for marginal rays passing through the objective lens. When the immersion oil and the cover glass are index matched which occurs for conventional immersion oils (dotted line in Fig.1),  $\theta_1$  and  $\theta_2$  can be easily calculated as 60.4° and 83°, respectively (NA=1.32= $n_1 \sin \theta_1$  and  $n_1 \sin \theta_1 = n_2 \sin \theta_2$  with  $n_1 = 1.518$  and  $n_2 = 1.33$ ). In this case the only component of the phase factor arising from glass-water interface can be written as  $\psi_{gw} = -0.59k_0 d_w$ , where  $d_w$  is the nominal depth of focus in the water medium and hereafter will be called trapping depth. In the case where the immersion oil and the glass are not index matched, this introduces an additional phase component which can be calculated in same manner. Increasing the refractive index of the immersion oil by  $\Delta n = 0.01$  implies  $\theta_0 = 59.7^\circ$  (fig.1), thus, the second component of the phase factor can be written as  $\psi_{og} = 0.021k_0 d_o$ , where  $d_o$  is the thickness of the oil layer. This thickness can be experimentally measured as the distance between the position at which the inner surface of the coverslip is in focus till the position at which the objective hits the sample. For our ITLC objective  $d_o$  was measured to be  $(115 \pm 15) \mu\text{m}$ , the uncertainty mainly arising from the variation in cover glass thickness. The optimal depth



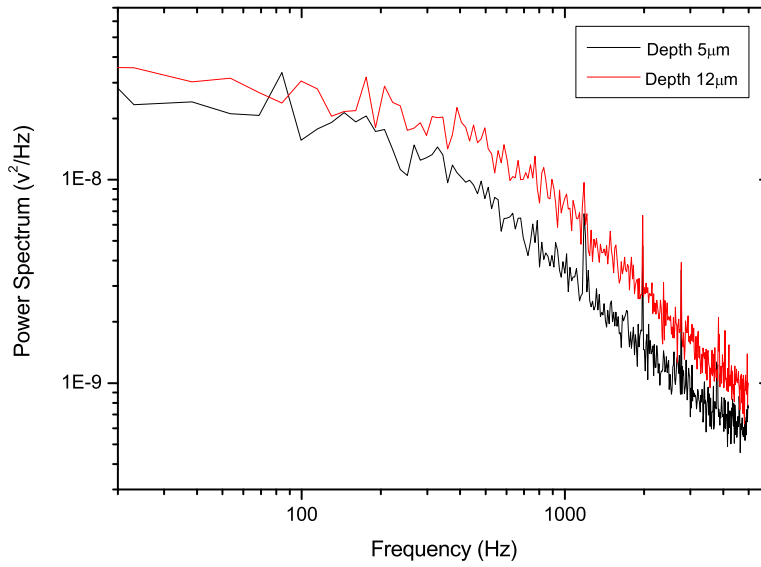
**Figure 1.** Schematic drawing of marginal rays (taken from reference.<sup>15</sup>  $d_o$ ,  $d_g$ ,  $d_w$  and  $d'_w$  denote the oil thickness, coverglass thickness, nominal trapping depth and actual trapping depth, respectively.



**Figure 2.** Axial spring constant as a function of trapping depth for polystyrene beads with a diameters of  $1.01 \mu\text{m}$  using a conventional immersion oil ( $n=1.518$ ).

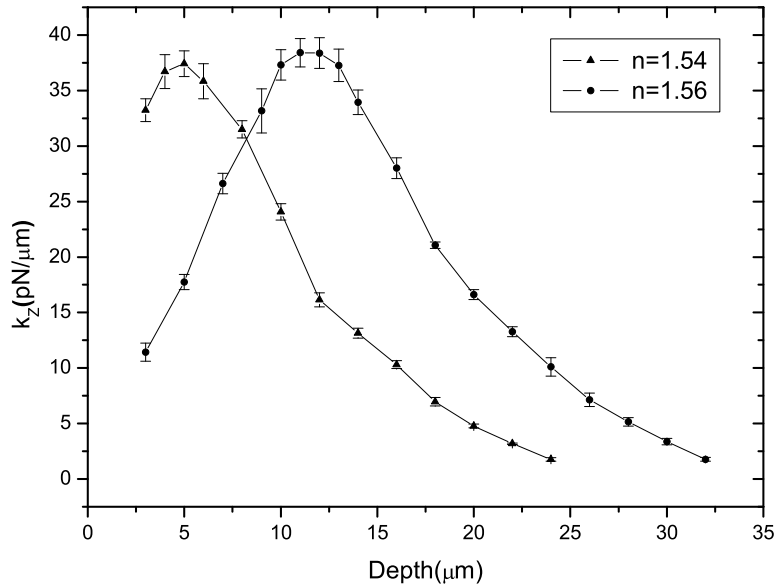
for optical trapping is the depth where these sources of spherical aberrations cancel, e.g. where  $\psi_{gw} + \psi_{og} = 0$ , which gives an optimal trapping depth of  $d_w = 4.1 \pm 0.5 \mu\text{m}$ . In other words, for the ITLC objective an increase of 0.01 in the refractive index of the immersion oil moves the optimal trapping depth  $(4.1 \pm 0.5) \mu\text{m}$  deeper into the sample.

Figure 2 shows the axial spring constant of the trap as a function of trapping depth using standard conditions: Polystyrene beads with diameters of  $1 \mu\text{m}$  (PS04N, Bangs Lab) diluted in distilled water were trapped using the ITLC objective lens and an immersion oil with refractive index,  $n=1.518$ , which is a standard immersion oil, typically recommended by the manufacturer. As the trapping depth increases aberrations also increase and the trap becomes less stable in the axial direction. At a depth of  $10 \mu\text{m}$  the Brownian motion of the bead overcomes the trapping forces and the bead escapes. Note that the trapping strength is monotonically decreasing away from the surface, there is no maximum. This is because the objective is optimized for visible and not for infrared wavelengths.



**Figure 3.** Typical power spectra of axial position signal for a  $1 \mu\text{m}$  polystyrene bead recorded at two different depths using an immersion media with  $n=1.56$ . The corner frequency, as well as the signal to noise ratio, increases with increasing trapping depth.

To show how the value of the refractive index affects the stability of the trap we performed a series of experiments using the ITLC objective with immersion oils with refractive indices of 1.54 and 1.56 (Cargille, Refractive index liquids set A). The experimental conditions were as for the data depicted in Figure 2. Between experiments with different immersion oils the objective was carefully cleaned and the chamber was replaced. The result of changing immersion oil is shown in Figures 3 and 4. Also, the results can be compared to Figure 2, where the same experiment is shown using a conventional immersion oil with  $n=1.518$ . The results of using a larger variety of  $n$  are shown in reference [15]. Figure 3 shows a typical power spectrum of the axial position signal for two different depths for  $n=1.56$ . It is clear that as the depth changes the corner frequency and thus the spring constant of the trap changes. Also, the signal to noise increases. Figure 4 illustrates that: *i*) As the refractive index of the immersion oil increases the optimal trapping depth also increases. An 0.01 increment in refractive index gives rise to a shift of about  $4 \mu\text{m}$  in compensation depth; *ii*) The graphs corresponding to different immersion oils have nearly the same value of maximum spring constant and more or less appear to be horizontal shifts of each other. Therefore, one can consider the trap at the optimal trapping depth as nearly



**Figure 4.** Axial spring constant as a function of trapping depth for two different immersion oil refractive indices. The beads were of polystyrene with a diameter of  $1.01 \mu\text{m}$ .

aberration free. Also, this shows that if one wishes to perform an experiment at a given depth within the sample, it is important to choose the correct immersion oil to have an efficient optical trap. By comparing Figure 2 to Figure 4 it is also evident, that one significantly improves optical trapping strength by optimizing the refractive index of the immersion media: The highest spring constant achievable using the conventional immersion media was  $12 \text{ pN}/\mu\text{m}$  whereas one easily obtains  $38 \text{ pN}/\mu\text{m}$  using the improved method. An improvement of 300 percent!

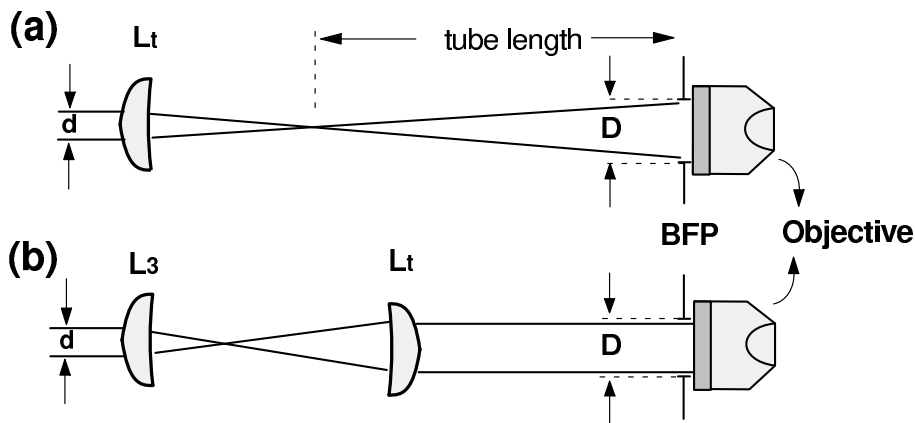


**Figure 5.** A sketch of focussing obtained by finite (a) and infinite (b) tube length settings. In (a) the laser beam at the back focal plane (BFP) is divergent, in (b) it is parallel.  $L_t$  is the tube lens, typically built into the microscope.  $L_3$  is a focussing lens.

It is known that alteration of the tube length is a different way to introduce or compensate spherical aberrations.<sup>4,9</sup> The definition of the tube length as well as the beam shapes at the entrance of the objective are

shown in Fig.5. Changing the tube length corresponds to using an FTLC objective in a microscope intended for an ITLC objective. Hence, we performed the tube length changing experiments using an FTLC objective in a microscope intended for ITLC objectives. Experiments were performed with two different sizes of beads,  $1\mu\text{m}$  and  $0.49\mu\text{m}$ . The magnitude of the lateral spring constant as a function of trapping depth is shown for two different sizes of beads in Figure 6. The immersion oil was the conventional with  $n=1.518$ . Comparing Figure 6 to Figure 2, where the same immersion oil was used, it is clear that using this different objective causes a maximum of trapping strength to appear at a particular trapping depth (at  $50\text{-}60\mu\text{m}$  depending on the diameter of the particle). Also, the magnitude of the spring constant is considerably larger despite the fact that the same immersion oil was used. Using a particle with diameter  $1\mu\text{m}$  gave nearly identical behavior of the lateral spring constant in the two measured directions,  $x$  and  $y$ , which follow the  $s$  and  $p$  polarization directions of the laser light, respectively. However, using a smaller bead with diameter  $0.49\mu\text{m}$  gave significantly different spring constants in the two lateral directions, with the  $y$  direction being more sensitive to aberrations. This confirms that the anisotropy of the trap is size dependent.<sup>14</sup>

As mentioned earlier, one problem with using the immersion oil for tuning the compensation depth is that its aberration effects can not be varied continuously but only discretely. However, a combination of changing immersion oil with changing tube length (e.g. by a movable lens inside the microscope) will provide a continuous way of tuning the compensation depth over hundreds of microns within the sample. Figure 7 illustrates this principle. It shows a combination of the FTLC objective with different immersion oils, the indices of refraction of the immersion oils are so low that they would have caused the optimal trapping depth to appear for negative  $z$  values (as e.g. shown in Figure 2). We observed: *i*) That the optimal compensation depth for an  $n=1.52$  immersion oil used with an FTLC objective occurs at depth of about  $52\mu\text{m}$  which is very close to the optimal compensation depth shown in Figure 6 for lateral directions. *ii*) A reduction in the refractive index of the immersion oil (from the 'conventional' value of 1.518) can shift the compensation depth, such that e.g. an immersion oil of  $n=1.46$  combined with the FTLC objective almost reproduces the graph shown in Figure 2 for the ITLC objective and  $n=1.518$  oil. *iii*) Further increasing the refractive index of the immersion oil will probably give rise to a further increase of the compensation depth. *iv*) A decrement of 0.01 of the immersion oil refractive index shifts the compensated depth by  $\sim 10\mu\text{m}$  for the experiment using an FTLC objective.

In conclusion, we have combined a change of immersion oil with changing the tube length. This has resulted in a continuous way of changing the optimal trapping depth. The present results are obtained by a combination of two previously published methods, namely that of changing immersion oil,<sup>15</sup> where an increment (decrement) of 0.01 in refractive index of the immersion oil gives rise to a increase (decrease) of about  $4\mu\text{m}$  and  $10\mu\text{m}$  in the compensation depth of the trap for ITLC and FTLC objectives, respectively. Also, this method provides a way to increase the axial strength of an optical trap by approximately a factor of three. The other method which was used was to change the tube length.<sup>4,9</sup> The physical mechanism behind the two methods is to introduce new spherical aberrations and hence compensate for those aberrations which are un-avoidable in an optical tweezers setup using commercially available objectives and infrared lasers. The present results devise a continuous and flexible way to tune the optimal trapping depth to accommodate specific wishes. Also, it shows how to trap objects deeper in the chamber than achieved by conventional optical tweezers.

The authors acknowledge financial support from the Villum Kann Rasmussen foundation.

## REFERENCES

1. S. N. S. Reihani and L. B. Oddershede, "Optimizing immersion media refractive index improves optical trapping by compensating spherical aberrations", *Opt. Lett.*, **32**, 1998 (2007).
2. A. Ashkin, J.M. Dziedzic and T. Yamane, *Nature* **330**, 769 (1987).
3. W.M. Lee, B.P.S.Ahluwalia, X.-C. Yuan, W.C. Cheong and K. Dholakia, "Optical steering of high and low index microparticles by manipulating an off-axis optical vortex," *J. Opt. A* **7**, 1 (2005).
4. S.N. S.Reihani, M.A. Charsooghi, H.R. Khalesifard and R. Golestanian, *Opt. Lett.* **31**, 766 (2006).
5. T. M. Hansen, S. N. S. Reihani, L. B. Oddershede and M. A. Sørensen, "Correlation between mechanical strength of messenger RNA pseudoknots and ribosomal frame shifting", *PNAS*, **104**, 5830 (2007).
6. C. Bustamante, Z. Bryant and S.B. Smith, "Ten years of tension: single-molecule DNA mechanics," *Nature* **421**, 423 (2003).

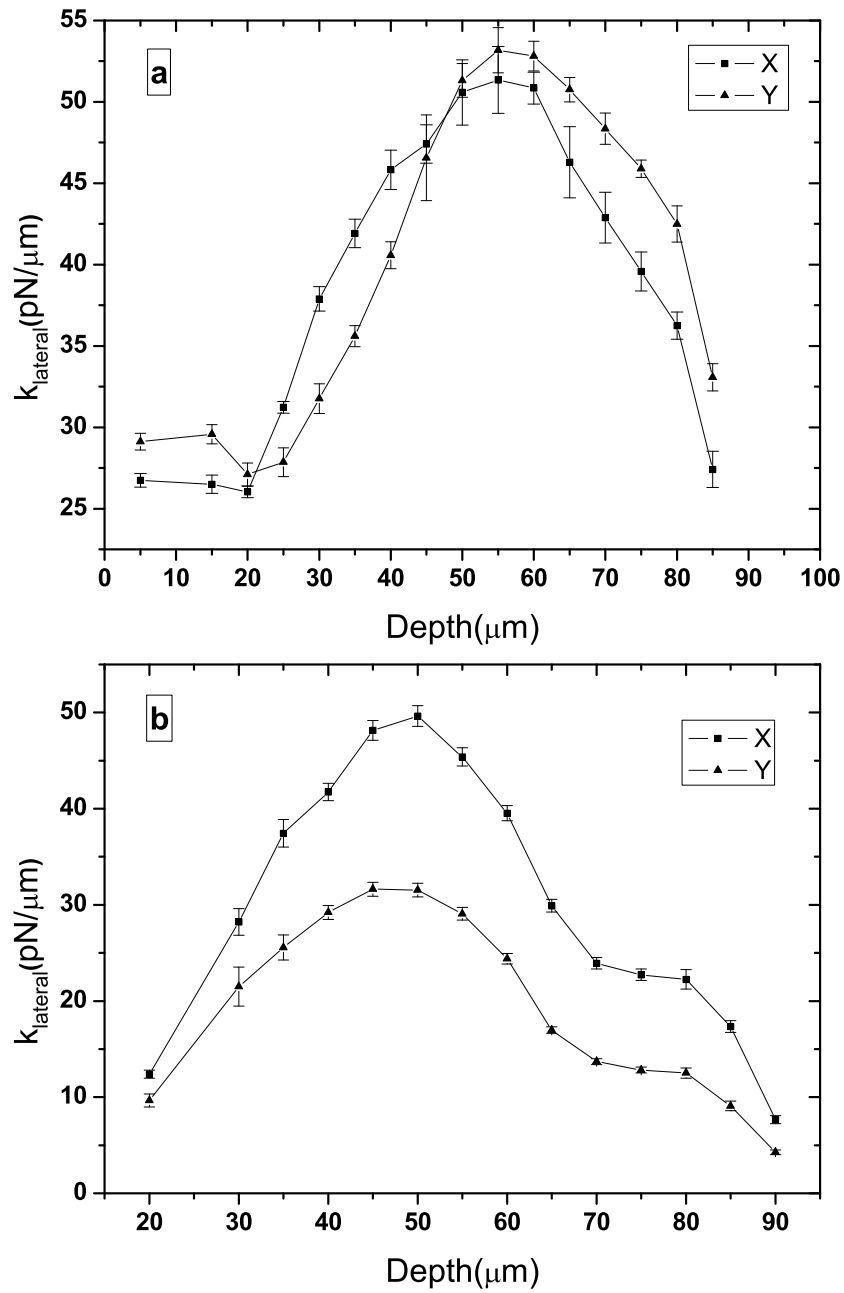


**Figure 6.** Shift in compensation depth caused by using the FTLC objective (tube length=170mm) in an infinity corrected microscope (corresponds to changing tube length). Lateral spring constant versus trapping depth for a)  $1\ \mu\text{m}$  and b)  $0.49\ \mu\text{m}$  polystyrene beads. The refractive index of immersion oil is  $n=1.518$ .

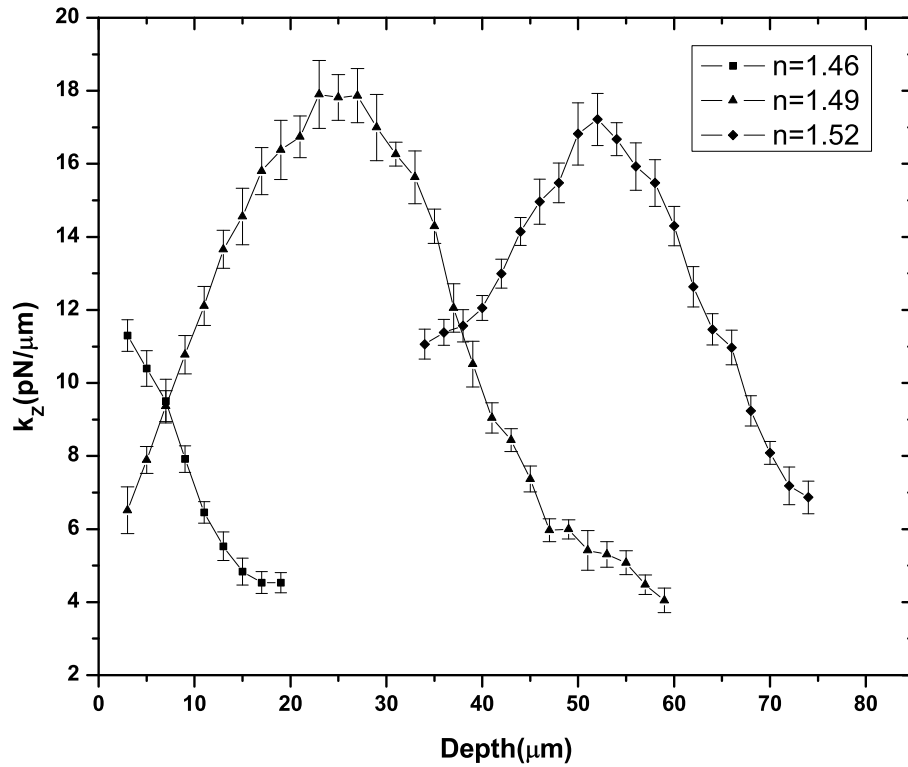


**Figure 7.** Axial spring constant as a function of trapping depth. This figure shows the effect of using a combination of an FTLC objective (tube length=170mm) in an infinity corrected microscope with different immersion oils, thereby introducing two sources of aberrations. Beads were 1 $\mu$ m polystyrene beads. The output laser power was 300mW.

7. C.J.R. Sheppard, M. Gu, K. Brain, H. Zhou " Influence of spherical aberration on axial imaging of confocal reflection microscopy," *Appl. Opt.* **33**, 616 (1994).
8. P.C. Ke, M. Gu " Characterization of trapping force in the presence of spherical aberration," *J. Mod. Opt.* **45**, 2159 (1998).
9. S.N.S. Reihani, H.R. Khalesifard and R. Golestanian, *Opt. Comm.* **259**, 204 (2006).
10. F. Gittes and C. F. Schmidt, "Interference model for back-focal-plane displacement detection in optical tweezers", *Opt. Lett.* **23**, 7 (1998).
11. L. Oddershede, S. Grego, S. Nørrelykke and K. Berg-Sørensen, *Probe Microscopy*, **2**, 129 (2001).
12. K. Berg-Sørensen and H. Flyvbjerg, *Rev. Sci. Ins.*, **75**, 594 (2004).
13. J. K. Dreyer, K. Berg-Sørensen, and L. Oddershede, "Improved axial position detection in optical tweezers measurements", *Appl. Opt.*, **43**, 1991 (2004).
14. A. Rohrbach, "Stiffness of the optical traps: Quantitative agreement between experiment and electromagnetic theory", *Phys. Rev. Lett.*, **95**, 168102 (2005).
15. S. N. S. Reihani and L. B. Oddershede, " Optimizing immersion media refractive index improves optical trapping by compensating spherical aberrations", *Opt. Lett.*, **32**, 1998 (2007).